Generation–recombination noise in extrinsic photoconductive detectors

Thomas J. Brukilacchio and Mark D. Skeldon

The Institute of Optics, University of Rochester, Rochester, New York 14627

Robert W. Boyd

The Institute of Optics and C.E.K. Mees Observatory, University of Rochester, Rochester, New York 14627

A theory of generation–recombination noise is presented and applied to the analysis of the performance limitations of extrinsic photoconductive detectors. The theory takes account both of the photoinduced generation of carriers and of thermal generation that is due to the finite temperature of the detector. Explicit formulas are derived that relate the detector response time, responsivity, and noise equivalent power to the material properties of the photoconductor (such as the presence of compensating impurities) and to the detector's operating conditions, such as its temperature and the presence of background radiation. The detector's performance is shown to degrade at high background levels because of saturation effects.

1. INTRODUCTION

There is currently great interest in extrinsic photoconductivity as a means of detecting far-infrared radiation for spectroscopic and astronomical applications. The dominant noise mechanism in photoconductive detectors is generation–recombination noise, which arises from the statistical fluctuations in the number of free carriers that are available to conduct current.[1-3] The simplest theories of generation–recombination noise assume that the detector responsivity and response time (i.e., excess carrier lifetime) are independent of the background radiation level to which the detector is exposed. In this case, it is well known that the background-limited noise-equivalent power (NEP) of the detector is $2^{1/2}$ times larger than that of an ideal photon detector, that is, a detector for which the only noise source is the fluctuations in the arrival times of the incident photons. The factor of $2^{1/2}$ arises from the independent fluctuations in the generation and recombination rates of the free carriers within the detector. The theory of generation–recombination noise as applied to extrinsic photoconductors can be far more complicated. In the far infrared, background photon fluxes can be large, even for backgrounds of relatively low temperature. At impurity concentrations normally employed, this background level can alter the carrier concentrations significantly from their thermal-equilibrium values. As a result, the detector responsivity, response time, and carrier fluctuations can differ greatly from their equilibrium values, leading to a NEP quite different from that predicted by the simple theories.

In this paper, we present a general theory of generation-recombination noise in extrinsic photoconductive detection systems. The calculation is based on a statistical method introduced by Burgess[4] in his treatment of generation–recombination noise in doped semiconductors. This approach applies detailed balancing to the carrier generation and recombination rates. The theory is thus capable of including the effects both of photogeneration of carriers and of thermal generation that is due to the finite temperature of the detector. The somewhat simpler thermodynamic treatment[4] of generation–recombination noise cannot be applied to photoconductors because in the presence of the radiation background the detector will not in general be in equilibrium. The effects of photon bunching[5] on the photogeneration rate are not included in the present theory; such effects can often be neglected under realistic operating conditions.[6]

Section 2 presents a treatment of the statistical properties of the photoconductive material. Impurity compensation of the majority carrier is addressed in this treatment and is shown to affect the noise properties of the detector. In Section 3, the results of this treatment are applied to analyze the performance limitations of an extrinsic photoconductive detector. Explicit formulas that relate the responsivity and the NEP to the detector's material parameters and to its operating conditions are derived. Our treatment goes beyond that of other recent workers[1-3] in that (1) the effects of compensating impurities are taken into account, (2) both thermal excitation and photoexcitation are included, and (3) our treatment can be used even in the presence of a large radiation background for which the fractional ionization of the impurity level is not small.

2. STATISTICS OF EXTRINSIC PHOTOCONDUCTIVITY

Let us consider the impurity photoconductor whose energy-level diagram is shown in Fig. 1. The photoconductor is assumed to contain N_d donor impurities and N_a acceptor impurities lying within the band gap. We assume that $N_d > N_a$, in which case the detector is known as an n-type extrinsic photoconductor. We assume that the temperature of the material is significantly low that band-to-band transitions can be ignored. Even in the absence of thermal generation or photogeneration, however, N_a of the donor levels will be ionized (i.e., vacant), since electrons can fall spontaneously
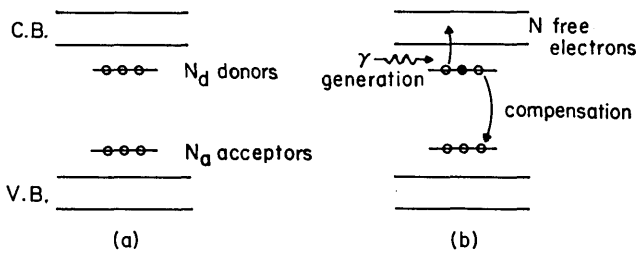
Fig. 1. (a) Energy-level diagram of an n-type ($N_d > N_a$) extrinsic photoconductor; (b) of the N_d donor electrons, a number N_a fall into the vacant acceptor levels. The remaining ($N_d - N_a$) electrons are available for excitation to the conduction band.

into the available acceptor levels. Hence only $N_d - N_a$ of the N_d donor electrons are available for excitation to the conduction band. In effect, N_a of the donor impurities are compensated for by the presence of the acceptors. It is thus useful to define the impurity-compensation ratio as

$$\lambda = N_a/N_d. \tag{1}$$

We define $N(t)$ to be the total number of electrons occupying the conduction band at time t. In general, $N(t)$ will be a fluctuating quantity. These fluctuations result from the randomness of the electron generation and recombination processes and are responsible for the noise (known as generation–recombination or g–r noise) in the photocurrent produced by the detector. In the present analysis, $N(t)$ is the only dynamical variable describing the detection system, since the donor-level population is always equal to $N_d - N_a - N(t)$. The properties of the two-level system composed of the donor level and conduction band are, however, quite different from those of the familiar two-level atomic system[7] In particular, we shall show that the rate at which $N(t)$ increases with incident power is quite different from the rate at which the population inversion of a two-level atomic system saturates with increasing power. Our calculation makes use of a method introduced by Burgess[4] in which detailed balancing is applied to the generation and recombination processes. We let $g(N)dt$ denote the probability that an electron is excited to the conduction band in a time dt if N electrons are already there. The generation rate $g(N)$ is assumed to be proportional to the number of un-ionized donors:

$$g(N) = \gamma(N_d - N_a - N). \tag{2}$$

The generation coefficient γ is assumed to be the sum of a thermal contribution that increases rapidly with temperature and a radiative contribution that increases linearly with photon flux. Similarly, $r(N)dt$ is defined to be the probability that one of the N electrons initially in the conduction band returns to the donor level in time dt. The recombination rate $r(N)$ is assumed to be proportional to the product of the number of free electrons and to the number of ionized donors as follows:

$$r(N) = \rho N(N_a + N). \tag{3}$$

The proportionality constant ρ is known as the recombination coefficient. Burgess has shown that ρ may be represented as $\langle v \rangle \langle s \rangle / \mathcal{V}$, where $\langle v \rangle$ is the mean thermal velocity of a conduction-band electron, $\langle s \rangle$ is the electron-capture cross section averaged over the electron velocity distribution, and $\mathcal{V}$ denotes the sample volume.

A master equation is now used to describe the time evolution of the probability $p(N)$ that the conduction band contains N free electrons:

$$\frac{d}{dt} p(N) = r(N + 1)p(N + 1)$$
$$+ g(N - 1)p(N - 1) - p(N)[g(N) + r(N)]. \tag{4}$$

In steady state, $dp(N)/dt = 0$, and this equation can be solved iteratively to obtain

$$\frac{p(N)}{p(0)} = \prod_{\nu=0}^{N-1} g(\nu) \Big/ \prod_{\nu=1}^{N} r(\nu). \tag{5}$$

An expression for $\overline{N}$, the most probable value of N, is obtained by treating N as a continuous variable and setting $dp(N)/dN$ equal to zero. For $\overline{N} \gg 1$, the resulting expression becomes

$$g(\overline{N}) = r(\overline{N}), \tag{6}$$

showing that in equilibrium the generation and recombination rates must balance. The form of the probability distribution $p(N)$ for N close to $\overline{N}$ can be shown[4] to be the Gaussian distribution

$$p(N) = p(\overline{N})\exp\left[\frac{-(N - \overline{N})^2}{2(\Delta N)^2}\right], \tag{7}$$

where the variance of N is given by

$$\overline{(\Delta N)^2} = g(\overline{N})\tau, \tag{8a}$$

where

$$\tau = [r'(\overline{N}) - g'(\overline{N})]^{-1} \tag{8b}$$

can be interpreted as the detector response time. Equations (8) were first derived by Burgess[4] and are known as the g–r theorem.

The material properties of the photoconductor can be obtained from Eqs. (7) and (8). The mean number of electrons present in the conduction band can be obtained from Eq. (6) by using the assumed forms [Eqs. (2) and (3)] for $g(N)$ and $r(N)$, giving

$$\overline{N} = \frac{-1}{2}\left(\frac{\gamma}{\rho} + N_a\right) + \left[\frac{1}{4}\left(\frac{\gamma}{\rho} + N_a\right)^2 + \frac{\gamma}{\rho}(N_d - N_a)\right]^{1/2}. \tag{9}$$

It is convenient to express this result in terms of dimensionless variables. We define a dimensionless generation coefficient by

$$\Gamma = \frac{\gamma}{\rho N_d} \tag{10}$$

and the fractional ionization of uncompensated impurities by

$$f = \frac{\overline{N}}{N_d - N_a} = \frac{\overline{N}}{N_d}\left(\frac{1}{1 - \lambda}\right). \tag{11}$$

By combining Eqs. (1), (9), (10), and (11), we obtain

$$f = \left(\frac{1}{1 - \lambda}\right)\left\{\frac{-1}{2}(\Gamma + \lambda) + \left[\frac{1}{4}(\Gamma + \lambda)^2 + \Gamma(1 - \lambda)\right]^{1/2}\right\}. \tag{12}$$

The functional dependence of f on Γ is illustrated in Fig. 2 for the limiting values of $\lambda \equiv N_a/N_d$. Here it can be seen that for large values of the generation rate the fractional ionization
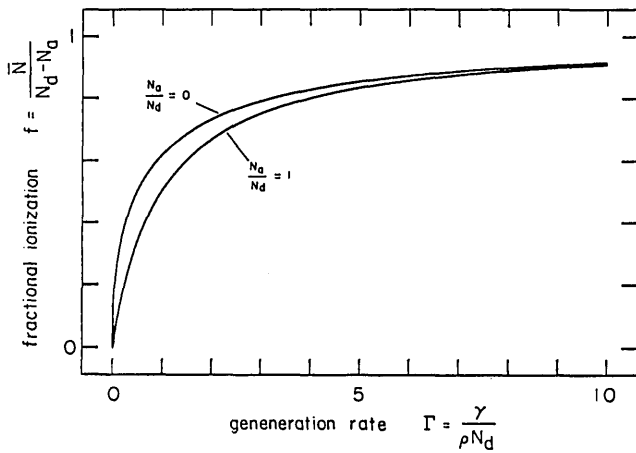
Fig. 2. Fractional ionization as a function of the generation rate.

approaches unity. In contrast, the maximum fractional population difference of a two-level atomic system is one half.

In general, the generation coefficient has both thermal and radiative contributions and can be represented as

$$\Gamma = \Gamma_{rad} + \Gamma_{th}. \tag{13}$$

An explicit expression for Γ_{th} can be obtained by comparing $\overline{N}$ from Eq. (9) with the standard result for the conduction-band electron density of a doped semiconductor that is in thermal equilibrium at temperature T.[8] This procedure yields the relation

$$\Gamma_{th} = \frac{V}{N_d}\frac{1}{2}N_c \exp(-E_d/kT), \tag{14}$$

where $-E_d$ is the energy of the donor level measured from the conduction-band edge and where N_c is the conduction-band density of states. For a parabolic band, N_c can be represented as

$$N_c = 2(2\pi mkT/h^2)^{3/2}, \tag{15}$$

where k denotes Boltzmann's constant, h denotes Planck's constant, and m denotes the effective mass of an electron. By using this result, the dimensionless generation rate can be expressed as

$$\Gamma_{th} = \Gamma_0 \left(\frac{kT}{E_d}\right)^{3/2} \exp\left(-\frac{E_d}{kT}\right), \tag{16}$$

where

$$\Gamma_0 = \frac{V}{N_d}\left(\frac{2\pi mE_d}{h^2}\right)^{3/2}. \tag{17}$$

Equation (16) shows how the thermal generation rate scales with the dimensionless temperature kT/E_d. This functional dependence is illustrated in Fig. 3. The proportionality constant Γ_0 depends on details of the material system, such as the doping level and donor ionization energy. For the sake of illustration, we consider the value of Γ_0 appropriate to a typical Ge:Ga photoconductor[9]: $E_d = 0.01$ eV and $N_a/V = 2.5 \times 10^{14}$ cm^{-3}, implying that $\Gamma_0 = 1.33 \times 10^4$. If one assumes this value of Γ_0, Eqs. (12) and (17) can be combined to yield the dependence of the fractional ionization on temperature. This dependence is illustrated in Fig. 4 for several different values of the compensation ratio $\lambda = N_a/N_d$. It can

be seen that the results do not depend critically on the compensation ratio. Figure 5 shows how the fractional ionization depends on the dimensionless temperature for a wide range of values of the material parameter Γ_0, assuming that $\lambda = 0$. These curves illustrate that the rate at which carriers freeze out depends strongly on the value of Γ_0.
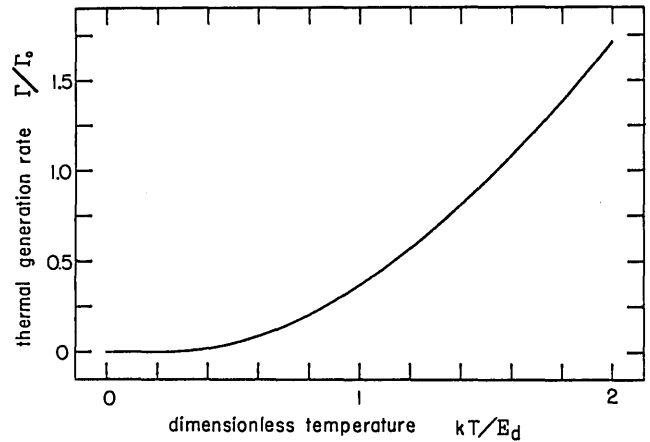

Fig. 3. Thermal generation rate $\Gamma = \Gamma_{th}$ as a function of the dimensionless temperature.
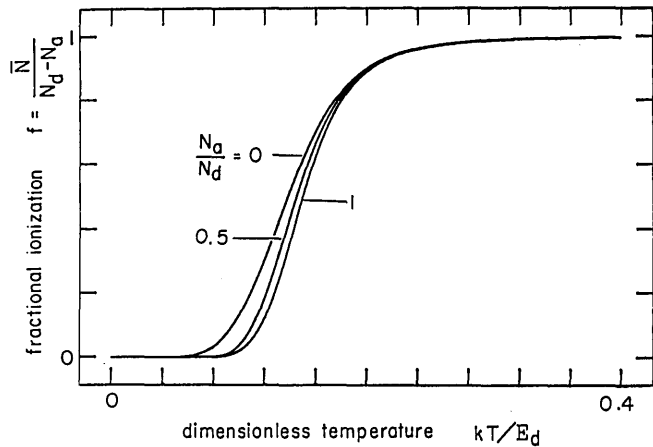

Fig. 4. Fractional ionization versus dimensionless temperature for several values of the compensation ratio assuming the value $\Gamma_0 = 1.33 \times 10^4$.
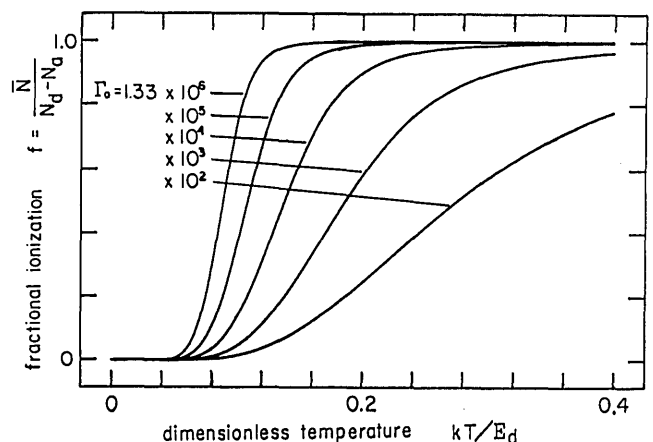

Fig. 5. Fractional ionization versus dimensionless temperature for $N_a/N_d = 0$.

The fluctuation in the total number of carriers can be obtained by using the g–r theorem given by Eqs. (8). Through differentiation of Eqs. (2) and (3) and use of Eq. (12), the detector-response time of Eq. (8b) can be expressed as

$$\tau = \frac{1}{\rho N_a} \frac{(1-f)\lambda}{f(2-f)(1-\lambda)+\lambda}.$$ (18)

This functional dependence is illustrated in Fig. 6. The mean-square carrier fluctuation can hence be obtained by using Eqs. (2), (8a), (9), and (18):

$$\overline{(\Delta N)^2} = N_d \frac{f(1-\lambda)(1-f)[\lambda+f(1-\lambda)]}{f(2-f)(1-\lambda)+\lambda}.$$ (19)

This functional dependence is illustrated in Fig. 7 for several values of the compensation ratio. Similarly, the dependence of the carrier fluctuation on the generation rate can be obtained from Eqs. (12) and (19). This dependence is illustrated in Fig. 8.

From a theoretical point of view, there is some interest in considering not the total mean-square fluctuation but rather this quantity divided by the mean number of carriers. From Eqs. (9) and (19) this ratio can be expressed as

$$\frac{\overline{(\Delta N)^2}}{\overline{N}} = \frac{(1-f)[\lambda+f(1-\lambda)]}{f(2-f)(1-\lambda)+\lambda}.$$ (20)
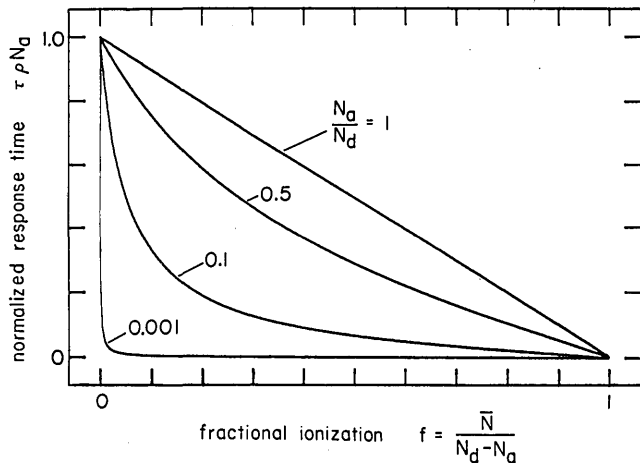

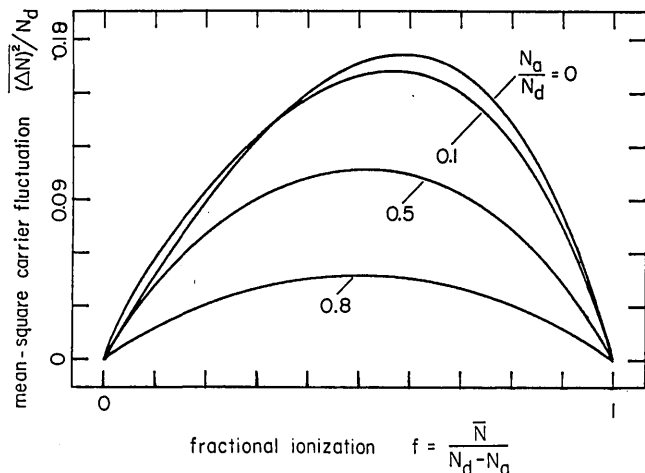Fig. 6. Normalized response time versus fractional ionization.

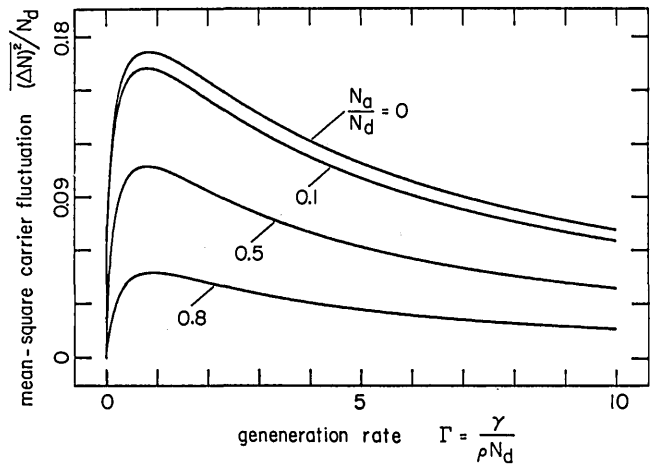Fig. 7. Mean-square carrier fluctuation versus fractional ionization.

Fig. 8. Mean-square carrier fluctuation versus generation rate.
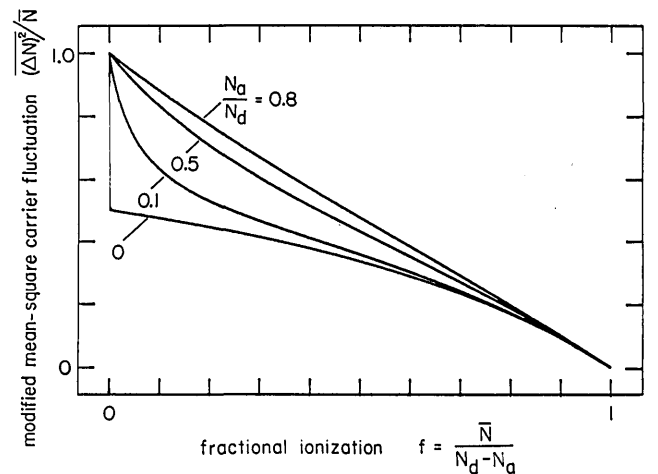

Fig. 9. Modified mean-square carrier fluctuation versus fractional ionization.

This ratio can be interpreted as a measure of the degree to which the fluctuations are Poissonian in nature. If the electrons obeyed Poisson statistics, the ratio would be unity under all conditions. The actual functional dependence is illustrated in Fig. 9 for several values of the compensation ratio. In general, the ratio $\overline{(\Delta N)^2}/\overline{N}$ is less than unity, showing that the electron fluctuations have become correlated through the concentration-dependent generation and recombination rates given by Eqs. (2) and (3).

3. DETECTOR CHARACTERISTICS

In this section we make use of the results derived in Section 2 to calculate the performance characteristics of an extrinsic photoconductive detector. We consider a slab of semiconductor material $\mathcal{V} = AL$, where L is the distance between the electrical contacts, as shown in Fig. 10. We assume as in Section 2 that only the transport of free electrons need be considered. If a potential V is applied to the detector, the instantaneous current is given by

$$i(t) = \frac{eV}{L^2} \mu_n N(t),$$ (21)

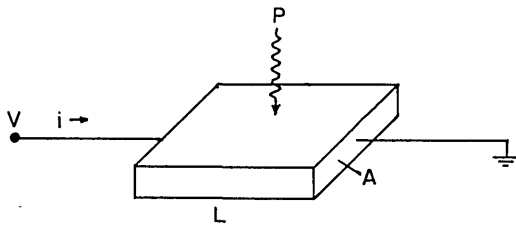where $N(t)$ denotes the total number of conduction-band

Fig. 10. Schematic photoconductive detector.

electrons at time t. The mean current passing through the detector is hence given by

$$\bar{i} = \frac{eV}{L^2}\mu_n \overline{N}. \tag{22}$$

The responsivity of a detector is defined to be

$$R = d\bar{i}/dP \tag{23}$$

where P denotes the optical power falling onto the detector. The treatment presented in Section 2 described the properties of the detector in terms of a generation coefficient γ defined by Eq. (2). This quantity is related to the power falling onto the detector by

$$\gamma = \eta P/h\nu(N_d - N_a), \tag{24}$$

where η denotes the detector quantum efficiency at low power levels, that is, in the absence of detector saturation effects. The detector responsivity can be expressed [using Eqs. (22)–(24)] as

$$R = \frac{\eta e V \mu_n}{h\nu L^2 (N_d - N_a)}\frac{d\overline{N}}{d\gamma}. \tag{25}$$

The derivative appearing here can be evaluated explicitly by using Eq. (9). This result can then be simplified by using the expression for γ/ρ obtained for Eqs. (2), (3), and (6):

$$\frac{\gamma}{\rho} = N_d \frac{f[\lambda + f(1 - \lambda)]}{(1 - f)}. \tag{26}$$

The responsivity can then be expressed as

$$R = \left(\frac{\eta e V \mu_n}{h\nu L^2}\right)\left(\frac{1}{\lambda \rho N_d}\right)\left[\frac{\lambda(1 - f)^2}{f(2 - f)(1 - \lambda) + \lambda}\right]. \tag{27}$$

The term in square brackets can be interpreted as a normalized responsivity and is plotted as a function of f in Fig. 11. The normalized responsivity is plotted [using Eq. (12)] as a function of generation rate in Fig. 12. This figure illustrates the rate at which the responsivity decreases because of saturation effects as the total generation rate Γ is increased either by increasing the detector temperature or by increasing the power incident upon the detector. Figure 13 illustrates how the responsivity at low power levels decreases as the temperature of the detector is increased. These curves were obtained using Eqs. (12), (16), and (27) and assuming the value $\Gamma_0 = 1.33 \times 10^4$.

The generation–recombination noise in the photocurrent can be expressed [using Eq. (21)] as

$$(\Delta i)^2 = \left(\frac{eV}{L^2}\right)^2 \mu_n{}^2 \overline{(\Delta N)^2}$$

$$= \frac{\bar{i}^2}{\overline{N}^2}\overline{(\Delta N)^2}, \tag{28}$$

where the second form results from the use of Eq. (22). This noise is composed of spectral components ranging from dc to

frequencies of the order of the inverse of the response time τ given by Eq. (18). In most detection systems, the electronics are designed so that only noise in a bandwidth $\Delta f \ll 1/\tau$ is present in the output signal. In this case, the current noise can be shown to be of the form[10]

$$\overline{i_{gr}{}^2} = 4\frac{\bar{i}^2}{\overline{N}^2}\overline{(\Delta N)^2}\tau\Delta f. \tag{29}$$
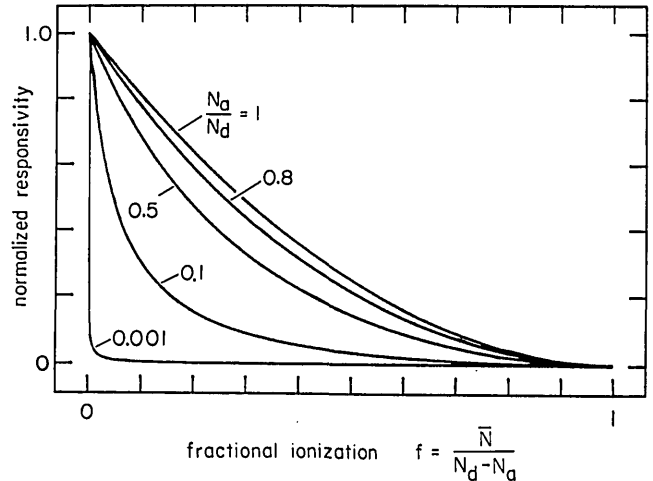

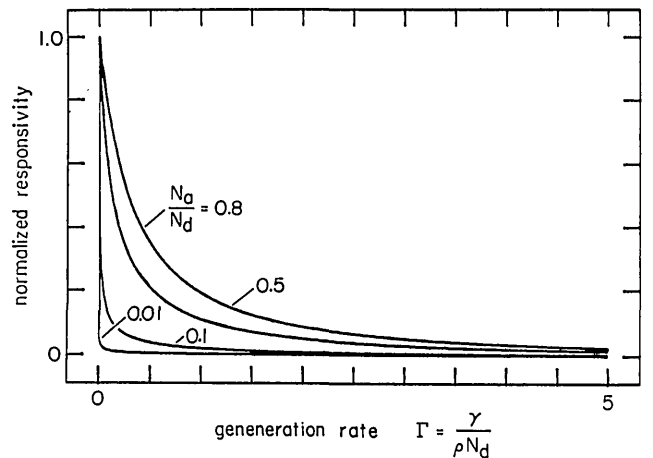Fig. 11. Normalized responsivity versus fractional ionization.

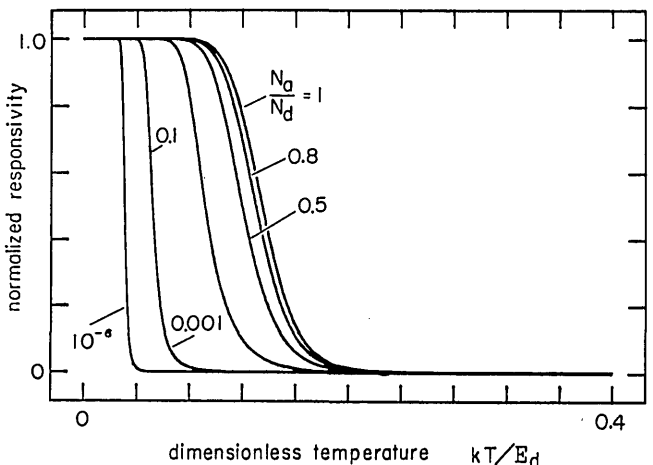Fig. 12. Normalized responsivity versus generation rate.

Fig. 13. Normalized responsivity versus dimensionless temperature.
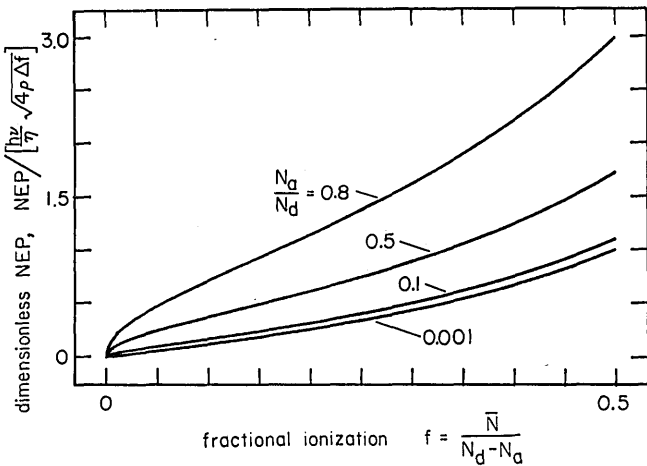
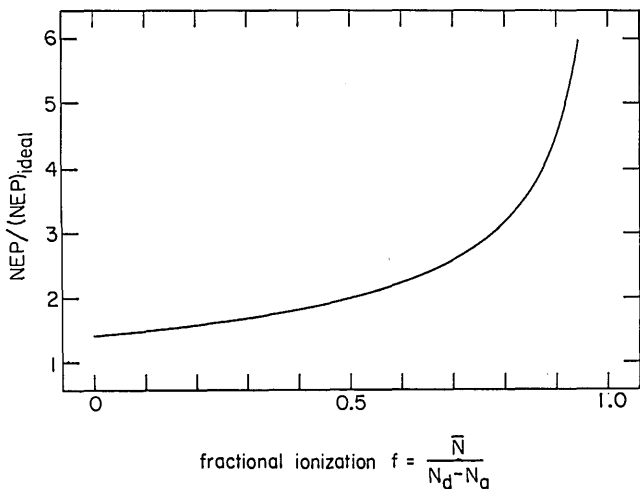Fig. 14. Dimensionless NEP versus fractional ionization.

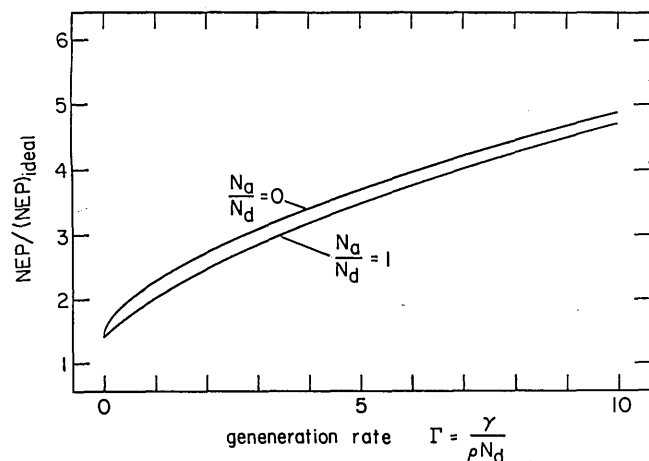Fig. 15. Normalized NEP versus fractional ionization.

Fig. 16. Normalized NEP versus generation rate.

A convenient descriptor of the noise properties of a detection system is the NEP, defined as the value of the signal power for which the signal-to-noise ratio is equal to unity. The NEP can be obtained generally from the relation

$$NEP = (i_{gr}^2)^{1/2}/R. \qquad (30)$$

Through use of Eqs. (18), (19), (27), and (29), the NEP can be expressed as

$$NEP = \frac{h\nu}{\eta} (4\rho\Delta f)^{1/2}(N_d - N_a) \left\{\frac{f[\lambda + f(1 - \lambda)]}{(1 - \lambda)(1 - f)^2}\right\}^{1/2}. \qquad (31)$$

This functional dependence is illustrated in Fig. 14. It is seen that the NEP increases with increasing fractional ionization.

It is well known that the lowest possible value of the NEP of a photodetector in the presence of a background power P_B is that imposed by photon shot noise and is given by the expression[10]

$$NEP_{ideal} = \left(\frac{2P_B h\nu\Delta f}{\eta}\right)^{1/2}. \qquad (32)$$

A convenient description of the noise properties of a photoconductor is hence given by the ratio of its NEP to that of an ideal photon detector. The ratio of Eqs. (31) and (32) can be simplified through use of Eqs. (24) and (26) to obtain

$$\frac{NEP}{(NEP)_{ideal}} = \left(\frac{2}{1 - f}\right)^{1/2}. \qquad (33)$$

This ratio is plotted as a function of the fractional ionization f in Fig. 15. We see that, for small values of f, the ratio approaches $2^{1/2}$. The value $2^{1/2}$ results from the fact that the generation and recombination processes are statistically independent, and each contributes noise to the detection process. At larger values of f, the ratio is larger, reflecting the decreased responsivity caused by a depletion of donor levels. In Fig. 16, we display the ratio $NEP/(NEP)_{ideal}$ as a function of the generation rate. These curves show the rate at which the NEP degrades as the radiation background is increased.

4. SUMMARY

A general theory of the statistical properties of extrinsic photoconductive detectors has been presented. Explicit formulas have been derived that show how the mean number of carriers, the mean-square fluctuation in this number, the detector response time, responsivity, and noise equivalent power depend on the temperature of the detector, the radiation background level, and the presence of compensating impurities. It has further been shown that, when the NEP is limited primarily by noise induced by the radiation background, the NEP is at least $2^{1/2}$ times larger than that of an ideal photon detector and that this limiting value is reached only if the fractional ionization of the donor level is small. The degradation of the NEP at higher background levels results from a decreased responsivity caused by a large fractional depletion of the donor impurities.

REFERENCES

1. The theory of generation–recombination noise is reviewed by D. W. Kruse, L. D. McGluchlin, and R. B. McQuistin, *Infrared Technology* (Wiley, New York, 1962); R. A. Smith, F. E. Jones, and R. P. Chasmar, *The Detection and Measurement of Infrared Radiation* (Oxford U. Press, London, 1968); R. J. Keyes and T. M. Quist, in *Infrared Physics*, Volume 5 of Semiconductors and Semimetals, R. K. Willardson and A. C. Beer, eds. (Academic, New York, 1970); D. Long, in *Optical and Infrared Detectors*, R. J. Keyes, ed. (Springer-Verlag, Berlin, 1977); R. W. Boyd, *Radiometry and the Detection of Optical Radiation* (Wiley, New York, 1983).
2. K. M. van Vliet, Proc. IRE **46**, (1958); Appl. Opt. **6**, 1145 (1967).
3. D. Long, Infrared Phys. **7**, 121 (1967); **7**, 169 (1967).
4. R. E. Burgess, Physica **20**, 1007 (1954); Proc. Phys. Soc. London Sect. B **68**, 661 (1955); Proc. Phys. Soc. London Sec. B **69**, 1020 (1956).
5. C. T. J. Alkemade, Physica **25**, 1145 (1959); G. W. Kattke and A. van der Ziel, Physica **49**, 461 (1970); K. M. van Vliet, Physica **83B**, 52 (1976).
6. R. W. Boyd, Infrared Physics **22**, 157 (1982).
7. L. Allen and J. H. Eberly, *Optical Resonance and Two-Level Atoms* (Wiley, New York, 1975).
8. See R. A. Smith, *Semiconductors* (Cambridge U. Press, Cambridge, 1978); J. S. Blakemore, *Semiconductor Statistics* (Pergamon, London, 1962).
9. Ge:Ga is in fact a p-type extrinsic photoconductor. The theory presented here has assumed the case of an n-type photoconductor because it is often easier to visualize the motion of electrons than that of holes. The theory developed here applies to a p-type photoconductor by formally interchanging the roles of the donor and acceptor levels and of the conduction and valence bands.
10. R. W. Boyd, *Radiometry and the Detection of Optical Radiation* (Wiley, New York, 1983), Chap. 10, especially p. 176.